J Mol Model (2008) 14:1173–1181
DOI 10.1007/s00894-008-0367-z

ORIGINAL PAPER

Density functional theory and Møller-Plesset studies of hindered rotations of acetone

M. Heidari · H. Rahemi · A. Tarashi · S. F. Tayarri

Received: 11 June 2008 / Accepted: 22 September 2008 / Published online: 16 October 2008

Abstract The hindered rotations of acetone were studied density functional theory (B3LYP) and second order Møller-Plesset approaches using 6-31G** and 6-311G** basis sets. One of the CH_3 groups of acetone with fixed heavy atoms was rotated from 0.0 to 120°, and CCH angles were scanned from 90.3 to 130.3° to cover the potential energy surface of interest; a circular valley was obtained with the deepest potential value at a CCH angle equal to 109.3°. Potential energy profiles were then calculated by assuming that the molecular geometry could relax during rotation (i.e., each value of the torsion angle of the molecular geometry was optimized). Next, the two methyl groups were both rotated clockwise, and then one was rotated clockwise and the other counterclockwise. Using the variation method, and utilizing the first 20 harmonic oscillator wave functions, the energy levels, relative transition moment and relative transition intensities of the component of the hindered rotation ν_2 (125.16 cm^{-1}) were computed in a one-dimensional Schrodinger equation. The first three energy levels were almost degenerate; the next three were opened up, and the seventh energy level appeared above the level where tunneling can occur.

Keywords Hindered rotation · Potential energy profiles · Potential energy surface · Torsion oscillation · Variation method infrared transitions

M. Heidari · H. Rahemi (✉) · A. Tarashi
Chemistry Department, Urmia University,
Urmia 57159-165, Iran
e-mail: hrahemi@yahoo.com

S. F. Tayarri
Chemistry Department, Ferdousi University,
Meshhad 91775-1436, Iran

Introduction

Acetone is used primarily as a chemical intermediate and as a solvent in both chemical and pharmaceutical applications. It is also very important in industrial and chemical reactions, being used as a raw material for the chemical synthesis of a wide range of products. The optimized structure of acetone with atomic numbering is given in Fig. 1.

Acetone is the molecular prototype for the aliphatic ketone series of molecules. In this molecule, the two methyl groups attached to the carbonyl are quite flexible, and are able to undergo torsional oscillation. Barriers that restrict such movement are known to be relatively low in this molecule, and thus the two CH_3 groups undergo internal rotation. As the rotors are attached to the same carbon atom, the hydrogen atoms of the methyl groups come into proximity, and can sterically interfere, with each other. The low frequency dynamics of coupled methyl rotors have been the subject of extensive review. As the torsion motions extend over large amplitudes, it is necessary to consider the complete potential energy surface (PES) defined by 360° rotations of the two torsion angles [1–3].

The microwave spectrum of acetone was first studied by Swalen and Costain [4] and later by Peters and Dreizler [5]. From the rotational spectrum patterns, these authors were able to determine an effective barrier for internal rotation. Vacherand et al. [6] carried out a complete analysis over a wider spectral range and refined the effective barrier, V_{eff}= 266.09 cm^{-1}. The most detailed study of the spectrum was that of Groner et al. [7]. These authors were able to observe the splitting of the bands into their torsional components at 125.16, 102.92, and 92.9 cm^{-1} in the infrared active $\nu_{17}(b_1)$ band while considering C_{2v} symmetry.

The aim of this paper was to study (1) the complete PES, where the CH_3 group is rotated internally by 360° and

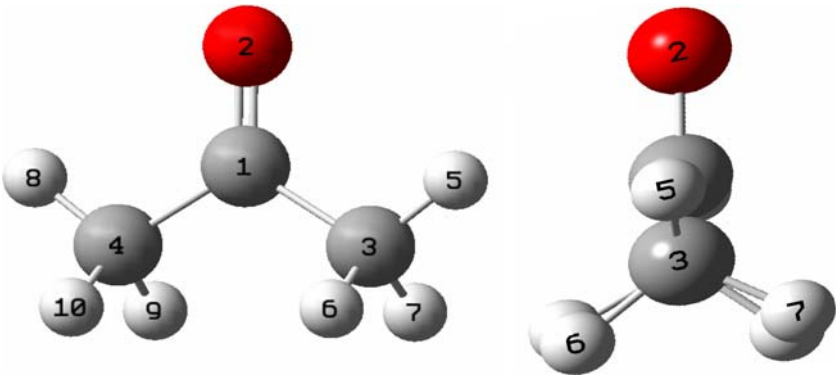

Fig. 1 Second order Møller-Plesset (MP2)/6-311G** optimized structure of acetone

makes an umbrella motion (C–C–H angle change from 90.3° to 130.0°); (2) semi-rigid (all heavy atoms fixed, and only hydrogen atoms rotate at the most stable fixed angle of C–C–H, 109.3°) potential energy profiles (PEP); and (3) the most reliable fully relaxed (only the O–C–C–H dihedral angle is fixed and all bond lengths and bond angles are optimized) PEP. Having wells below the saddle points, we will be able, through Hamiltonian construction and using the one-dimensional Schrodinger equation and variation method, to calculate energy levels and wave functions. The energy values are used to predict the frequencies, and the wave functions to calculate transition moments and relative intensities of far infrared transitions. The splitting of the levels depends on the degree of restriction of the rotational motion. Thus, at the bottom of the well, levels split by torsion may be close together and degenerate, whereas at the top of the well, they will be widely separated. Three transitions are expected to approximate experimental values.

Computational details

Gaussian 03 W v.6.0 [7] was the computer program used, and all calculations were carried out at density functional theory (DFT) [8] and second order Møller-Plesset (MP2) [9] levels. The underlying DFT theory was the Khon and Sham approach to DFT, which uses a one particle Schrodinger equation and was performed using self consistent field (SCF) procedures. The Vosko, Wilk and Nusair (VWN) formula [10] was used for local density approximation for general gradient approximation (GGA) of the combination of Becke's three-parameter adiabatic connection exchange functional [11] with Lee-Yang-Parr correlation [12]; a list of B3LYP components was selected. The Møller-Plesset [13] approach was a second order perturbation theory. In both approaches, the large standard basis sets of 6-31G** and 6-311G** were used.

Results

Structural

First, the full optimization of acetone was carried out at the MP2 and B3LYP/31G** calculation levels without applying a symmetry option. The calculations showed that the molecule has C_{2v} symmetry (Table 1). One hydrogen atom of each methyl group, H5 and H8, lies in the O–C–C plane and eclipses the oxygen. In a 120° CH_3 rotation, the C–H bond length and C–C–H bond angle change to 0.0046 Å and 0.3376°, respectively, and the CH_3 internal rotation axis forms an angle of approximately 0.17° with the C–C bond. These changes are small, and all C–H bond lengths and all C–C–H and H–C–H bond angles could be considered the same. In this case, the CH_3 rotational axis lies along the C–C bond. With the new settings, the B3LYP/6-31G** calculation showed C–C–H=110.23°, H–C–H=108.70°, C–O=1.2158 Å, C–H=1.0943 Å and C–C=1.5201 Å, which were in better agreement with experimental values [14].

Next, optimizations were performed at MP2 and B3LYP/6-311G** levels of theory. The molecule turned out to optimize with C_1 symmetry; the hydrogen atom is no longer in the O–C–C plane, and the O–C–C–H dihedral angles are +8.5° clockwise and −8.5° counterclockwise of the methyl groups. A small barrier with a height of 3.8 cm^{-1} at the O–C–C–H dihedral angle of ± 0° appeared (Fig. 1). Thus, the experimental structural and vibration analysis based on C_{2V} symmetry considerations needs to be revised.

Potential energy surface

The PES for one CH_3 rotation was constructed by approximating the C–H bond length and C–C–H bond angles to be equal. The dihedral angles of H–C–C–O,θ_1, from 0.0 to120.0°, and C–C–H angles, φ, from 90.3 to 130.3°, were scanned at 1° steps; 4,961 single point calculations were completed. The constructed PES was

Table 1 Second order Møller-Plesset (MP2)- and B3LYP-optimized bond lengths and bond angles

	MP2/6-311G**		B3LYP/6-311G**		Experimental [10]
	C_{2V}	C_1	C_{2V}	C_1	
Bond length (Å)					
C1–O2	1.2167	1.2165	1.2074	1.2091	1.215
C1–C3	1.5176	1.5179	1.5179	1.5191	1.515
C1–C4	1.5176	1.5175	1.5179	1.5191	1.515
C3–H7	1.0901	1.0901	1.0868	1.0890	1.086
C3–H8	1.0947	1.0941	1.0923	1.0943	1.086
C3–H9	1.0947	1.0995	1.0923	1.0950	1.086
C4–H10	1.0901	1.0901	1.0868	1.0890	1.086
C4–H11	1.0947	1.0941	1.0923	1.0943	1.086
C4–H12	1.0947	1.0995	1.0923	1.0950	1.086
Bond angle (°)					
O2–C1–C3	122.002	122.022	121.768	121.772	121.800
O2–C1–C4	122.002	122.022	121.768	121.772	121.800
C3–C1–C4	115.997	115.956	116.463	116.457	116.400
C1–C3–H7	109.665	109.345	109.673	109.695	110.267
C1–C3–H8	110.003	110.591	110.417	110.835	110.267
C1–C3–H9	110.003	109.721	110.417	109.963	110.267
C1–C3–H8	109.665	109.345	109.673	109.695	110.267
C1–C3–H9	110.003	110.591	110.417	110.835	110.267
C1–C3–H10	110.003	109.721	110.417	109.963	110.267
O2–C1–C3–H5	0.0	8.5	0.0	6.0	0.0

projected on a flat equatorial plane; a net presentation and contour map are shown in Figs. 2 and 3, respectively. The circular valley in Fig. 2 (only one-third of the valley is presented) can be divided into two parts: the space over the saddle points (the most unstable configuration of acetone θ_1=45° having the highest structural energy), and the wells below the saddle points. In the space over the saddle points, the internal methyl group can rotate freely. Below the saddle points, where three wells are located, out-of-plane bending could occur (hindered rotation or torsion oscillations of the a_2 and b_1 type). C–C–H in-plane bending (umbrella bending) uses both spaces. The slice of potential energy in the radial direction crossing through the bottom of the well, which is in the Morse-type potential, is the potential energy of the one C–C–H in-plane bend. The motion could be considered as one-dimensional, and its potential energy could be introduced into the Schrödinger equation. At points below the saddle, torsion motions of methyl groups occurred in three wells. In the torsion oscillation, all three hydrogen atoms were moving clockwise and counterclockwise from their equilibrium position, in harmony. Of course, two methyl groups could be coupled to each other as clockwise–clockwise and clockwise–counterclockwise.

Semi-relaxed PEP

The steepest curve in the valley occurred at φ=109.3°. Three circular PEPs were constructed at constant φ and with fixed heavy atoms (O and C atoms). First, one of the methyl groups was rotated; the symmetrical barrier heights had values of MP2/6-311G** = 287.9 cm^{-1} and B3LYP/6-311G** = 277.6 cm^{-1}. Second, two methyl groups were rotated, both clockwise. The corresponding heights were 1,061.2 cm^{-1} and 941.3 cm^{-1} for MP2 and B3LYP, respectively. Third, one methyl group was rotated clockwise and the other counterclockwise; the barrier heights were 1,058.2 cm^{-1} and 941.3 cm^{-1} using MP2 and B3LYP with the same basis sets, respectively. The straightened potential energy profile closely obeyed a sinusoidal function $V = V_3(1-\mathrm{Cos}3\alpha)/2$, where V_3 is the internal rotation barrier, and the factor 3 was the internal rotation symmetry number. In order to compare calculated PEPs with the sinusoidal function, V_3 was set arbitrarily to 282 cm^{-1} for one methyl group rotation, and to 1,000 cm^{-1} for both methyl groups rotation (Fig. 4). The barrier height with both methyl groups rotated in the same direction was equal to one methyl group rotating clockwise and the other counterclockwise, but the width was narrower.

The barrier height of one methyl group rotation MP2/6-311G** (287.9 cm^{-1}) was considerably less than one-half of the barrier height of the two methyl group rotations MP2/6-311G** (clockwise-clockwise; 1,061.2 $cm^{-1}$and clockwise–counterclockwise; 1,058.2 cm^{-1}), which demonstrated that, if both rotors operate together, rotor coupling is important.

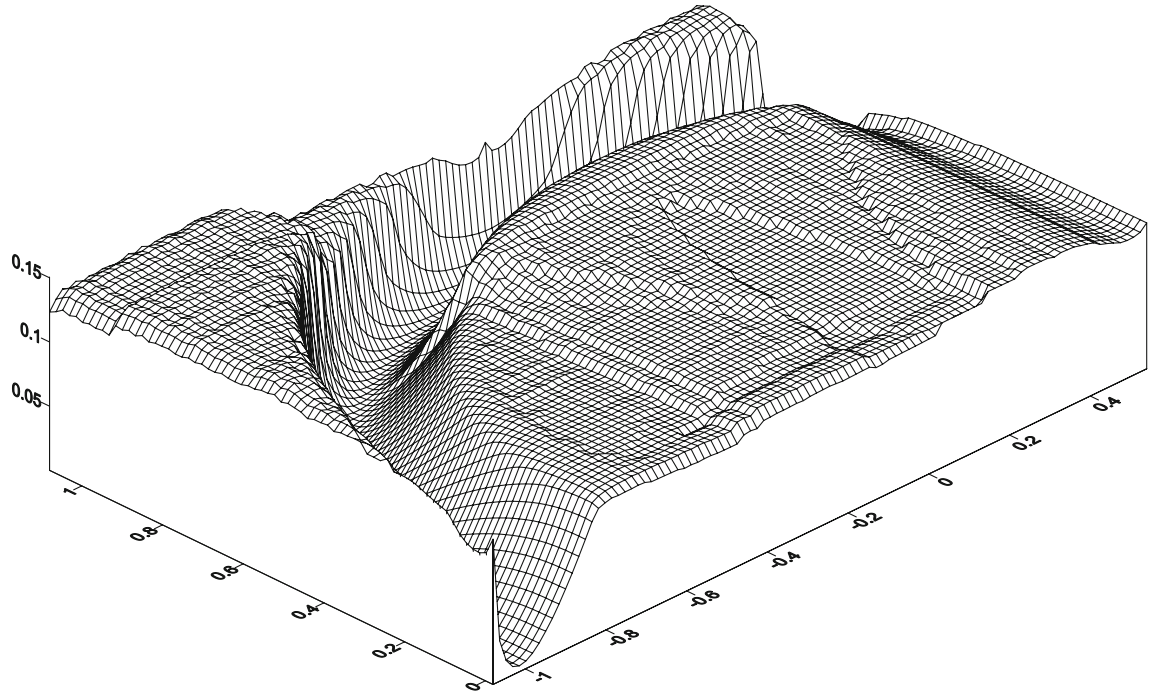

Fig. 2 Net representation of the projected potential energy surface (PES) on an equatorial plane. The circular valley represents the area of methyl internal motion. The cross-section shows the behavior of the anharmonic potential function, the steeper part reflects a small centrifugal distortion

Fully relaxed PEP

To obtain the most relaxed structure during the rotation, the potential energy as a function of the angle of rotation θ_1 and θ_2 (O2–C1–C3–H5 and O2–C1–C4–H8 dihedral angles, Fig. 1) was obtained by re-optimizing in steps of 2° from 0.0 to 120 at the proposed levels of calculation. The Z-Matrix was constructed in such a way that, by changing θ_1 and θ_2, other O–C–C–H dihedral angles change with the same 2° steps. In one methyl rotation, only θ_1, and in two methyl rotations, θ_1 and θ_2 were kept constant and all other structural variables were subjected to optimization (Fig. 5).

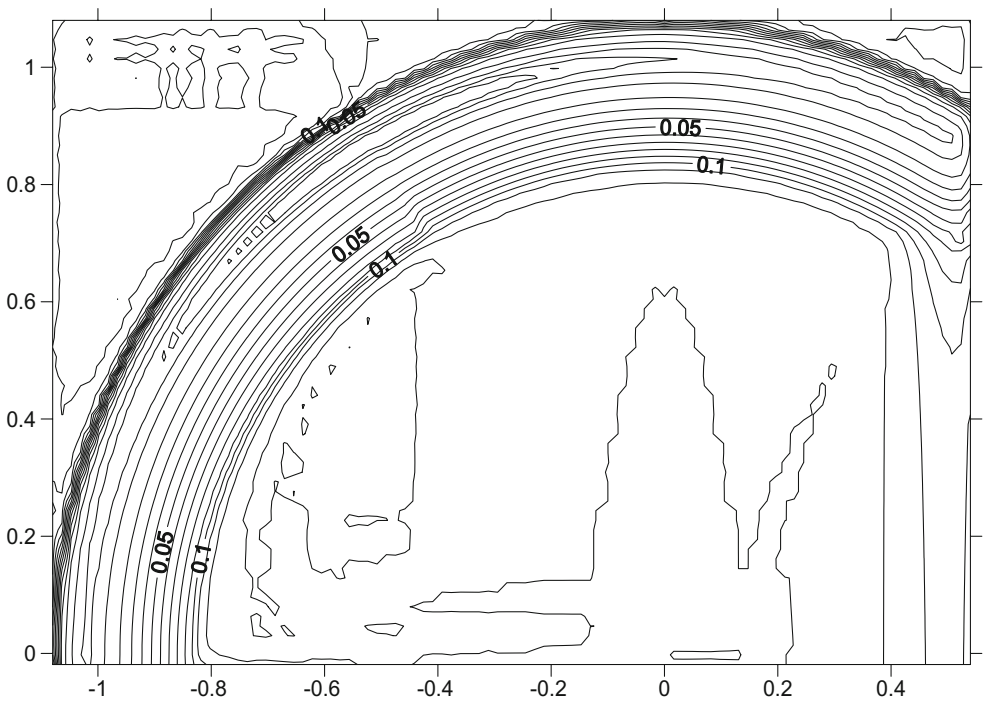

Fig. 3 Contour map, showing clearly the location of one well. The area outside the scan area is generated by the Surfur computer program and has no meaning

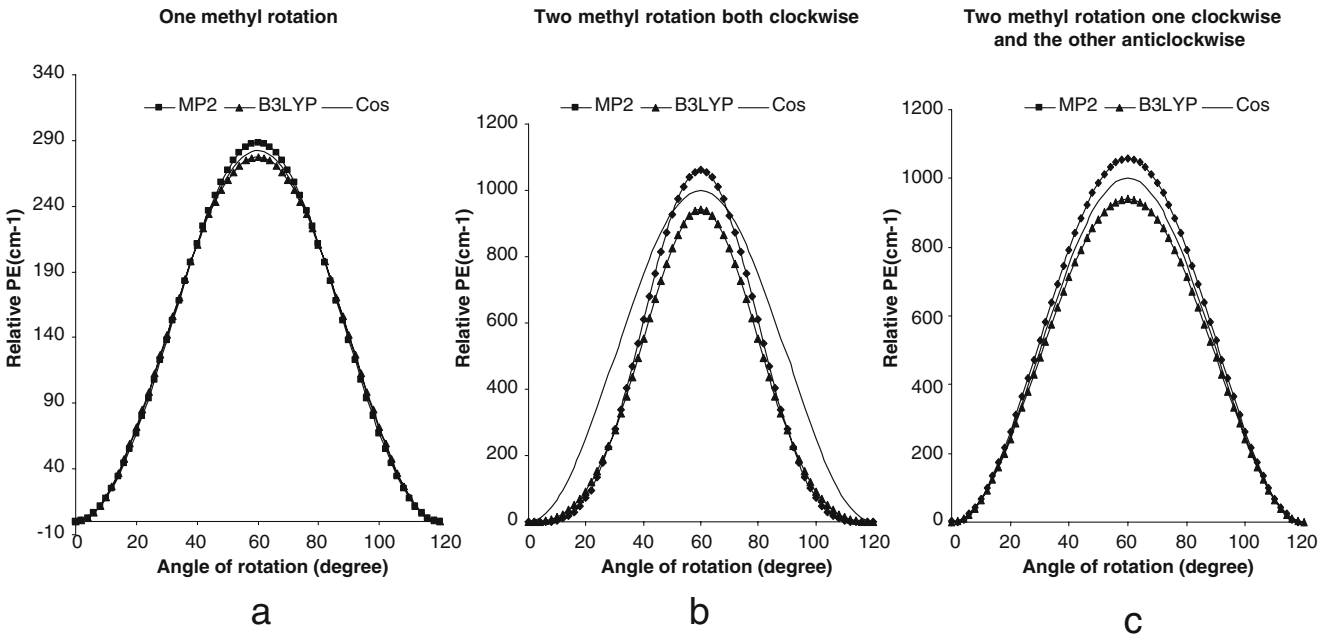

Fig. 4 **a** One methyl rotation, **b** two methyl rotation (both clockwise), **c** two methyl rotation (one clockwise and the other counterclockwise)

The PEP wells were wider while the barriers were narrower than the corresponding cosine potential, which provided relatively easier tunneling at the seventh energy level.

The fully relaxed model represented a more reliable approach to the torsion potential surface problem. An important outcome of this model was significant lowering of the torsion potential barrier to 233.0 cm^{-1} (B3LYP/6-31G**) and 265.6 cm^{-1}, (MP2/6-31G**), from the microwave 270 cm^{-1} value (Table 2). The hydrogen atom with $(1\ s)^1$ electronic structure was a simple atom, and in calculations it may be more convenient to use 6-31G** rather than more sophisticated basis functions such as 6-311G**. However, the second basis functions yield more detailed structure, and thus are more recommended.

An interesting point found using the fully relaxed model was that a small barrier occurred at θ_1=0.0°, whereas the most stable configurations (two configurations) appeared at θ_1=±6.0°, $\theta_2 = \mp 6.0°$and θ_1=±8.5°, $\theta_2 = \mp 8.5°$ for B3LYP and MP2, respectively. The could be because the angle of rotation was fixed and all other variables were optimized, which was found to be the most preferred optimization.

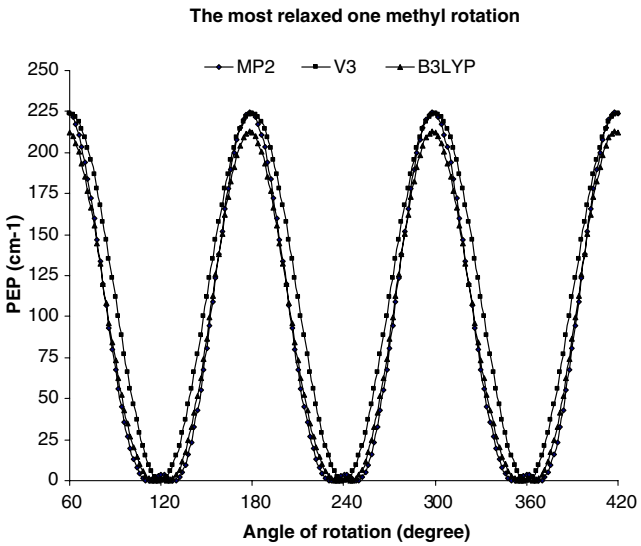

Fig. 5 The most relaxed one-methyl rotation, using MP2/6-311G** , V3 and B3LYP/6-311G** levels of calculations

Vibration

The fully optimized C_{2v} and C_1 structures at the most stable configuration, (θ_1=0.0° and θ_2=0.0° for both B3LYP and MP2) and (θ_1=±6.0° $\theta_2 = \mp 6.0°$ for B3LYP, and θ_1=±8.5° $\theta_2 = \mp 8.5°$ for MP2), were subjected to harmonic and anharmonic vibration frequency calculations using 6-311G** basis sets (Table 3). Apart from very low frequencies, MP2 values were closer to experimental values and, in the high region, B3LYP frequencies were a better match with the corresponding experimentally determined frequencies [15, 16]. Inspection of Table 3 reveals that the differences between harmonic and corresponding anharmonic frequencies are not a fraction number. A scaling factor could be used to convert harmonic to anharmonic frequencies, but more precautions may be needed in this case.

The CH_3 torsion—the vibration mode at 125 cm^{-1}—will be explored in depth because of its interesting triple split (125.2, 102.9, 92.9 cm^{-1}). We will take advantage of the

Table 2 Barrier heights computed with different structural settings and levels of theory (all in cm^{-1})

Barrier heights , CH_3 rotation	MP2		B3LYP		Experimental
	6-311G**	6-31G**	6-311G**	6-31G**	
Fully relaxed					
One CH_3 rotation	224.6	265.6	212.8	233.0	270
Both CH_3 clockwise rotation	797.0	784.8	705.0	724.0	
CH_3 clockwise and counterclockwise rotation	793.2	787.1	704.4	727.0	
Semi-relaxed					
One CH_3 rotation	287.9	322.5	277.6	291.7	270
Both CH_3 clockwise rotation	1,061.2	1,039.5	941.3	946.5	
CH_3 clockwise and counterclockwise rotation	1,058.2	1,039.5	941.3	946.5	

variation method to solve the Schrodinger vibration equation of the system.

The variation method

If a molecule can assume more than one stable configuration—in this case stable implies that the configuration is associated with the bottom of a potential well—we would have multiple well potentials. Such configurations are often equivalent and can be defined conveniently with a cosine function for each respective well. In the present case, the situation was more complicated. The internal rotation of methyl groups was previously thought to have three stable configurations, but our findings revealed that the molecule did not have a C_{2v} symmetry. Methyl groups in their stable configurations were rotated clockwise–counterclockwise about 8.5° leaving two stable conformations. Altogether six minimum PEPs (360°) were detected.

The dynamics, such as stretching, of a microscopic particle can be described with the one-dimensional Schrö-

Table 3 Vibrational band assignment of acetone (frequencies in cm^{-1})

No.	Assignment	B3LYP/6-311G** C_{2V}		B3LYP/6-311G** C_1		MP2/6-311G** C_{2V}		MP2/6-311G** C_1		Experimental [11, 12]
		Harmonic	Anharmonic	Harmonic	Anharmonic	Harmonic	Anharmonic	Harmonic	Anharmonic	
1	CH_3 torsion, a_2	-60.2	-48.7	56.2	-1056.1	-86.5	-164.8	79.3	-205.7	77
2	CH_3 torsion, b_1	114.8	139.8	139.0	8.8	127.2	117.2	139.0	139.6	125
3	C-C-C bend, a_1	373.0	390.1	377.3	380.6	375.2	378.3	376.7	385	385
4	CH_2 twist, b_1	491.8	494.0	488.9	476.8	488.4	486.2	481.4	485.2	484
5	Skeleton, b_2	528.3	528.6	535.6	530.0	533.6	529.5	534.4	531.5	530
6	C-Csym. str., a_1	783.7	767.7	779.2	766.4	804.0	787.2	803.5	789.3	777
7	CH_3 bend, a_2	885.7	884.8	882.6	856.8	889.5	882.8	889.1	861.2	877
8	CH_2 twist, b_2	892.8	877.1	884.0	826.6	898.4	885.8	906.1	877.1	891
9	CH_3 bend, a_1	1,082.1	1,068.8	1,083.1	1,051.8	1,087.6	1,065.0	1,091.3	1,070.5	1,066
10	CH_2 twist, b_1	1,125.8	1,099.2	1,117.3	1,095.9	1,127.3	1,100.0	1,121.2	1,101.4	1,091
11	C-C str. , b_2	1,234.7	1,202.3	1,230.3	1,194.8	1,252.1	1,217.8	1,253.9	1,220.9	1,216
12	CH_3umbrella bend, b_2	1,394.5	1,365.3	1,383.0	1,347.7	1,395.5	1,361.3	1,395.4	1,360.9	1,364
13	CH_3umbrella bend, a_1	1,397.5	1,368.6	1,385.5	1,343.5	1,404.1	1,368.7	1,405.8	1,368.6	1,364
14	CH2 wagg. , b_2	1,466.6	1,437.1	1,461.2	1,405.1	1,476.7	1,438.6	1,482.3	1,441.2	1,410
15	CH2 twist, a_2	1,475.6	1,445.9	1,466.3	1,425.2	1,485.8	1,449.5	1,486.2	1,448.7	1,426
16	CH2 wagg. , a_1	1,488.1	1,453.5	1,471.2	1,422.7	1,492.4	1,453.6	1,491.6	1,452.1	1,435
17	CH2 twist, b_1	1,509.6	1,477.2	1,488.2	1,433.1	1,513.0	1,472.1	1,506.8	1,461.7	1,454
18	C=O str. , a_1	1,822.9	1,797.0	1,804.2	1,780.9	1,787.4	1,728.2	1,787.7	1,740.0	1,731
19	CH_3sym. str. , a_1	3,047.1	2,947.9	3,024.5	2,908.8	3,079.0	2,977.8	3,075.3	2,974.1	2,937
20	CH_3sym. str. , b_2	3,053.0	2,954.0	3,031.3	2,918.3	3,083.4	2,981.5	3,080.0	2,979.2	2,937
21	CH_2 sym. str. , a_2	3,125.5	2,985.5	3,080.1	2,922.9	3,177.7	3,038.8	3,158.2	3,020.2	2,963
22	CH_2asym. str. , b_1	3,132.5	2,989.1	3,087.1	2,936.0	3,182.9	3,042.1	3,163.1	3,027.2	2,972
23	CH_3asym. str. , a_1	3,136.5	2,990.4	3,139.8	2,987.7	3,183.4	3,042.7	3,204.3	3,069.6	3,019
24	CH_3asym. str. , b_2	3,138.1	2,992.0	3,141.0	2,988.4	2,992.0	3,043.4	3,205.4	3,067.6	3,019

dinger equation. However, the potential energy function was complicated. Next, we attempted the variation method for the treatment of the problem, i.e., to treat the problem in one dimension, the circular hindered internal rotation potential was opened up and straightened.

Introducing the non-dimensional variables ξ and λ as [19]:

$$\xi = \left(\frac{\mu\omega_e}{h}\right)^2 R \quad \lambda = \frac{2E}{h\omega_e} \tag{1}$$

where $\hbar$ is Plank's constant divided by 2π, R is the variation in inter-nuclear distance, μ is the reduced mass of the involved nuclei, and ω_e is the arbitrary angular vibration frequency. In the ξ scale, the Schrodinger equation takes the following form:

$$\frac{d^2\Psi(\xi)}{d\xi^2} - \frac{2V(R)}{\hbar\omega_e}\Psi(\xi) = -\lambda\Psi(\xi) \tag{2}$$

where $V(R)$ is the potential energy of the torsion motion. Due to the lack of mathematical potential energy, a direct solution of Eq. 2 is not possible; therefore, the variation method will be applied. The wave function is expanded as:

$$\Psi(\xi) = \sum_{i=0}^{n} C_i\Phi_i(\xi) \tag{3}$$

where $\Phi_i(\xi)$ is simple harmonic oscillator wave function. The term H_{jk} is defined as:

$$H_{jk} = HK_{jk} + HU_{jk} \tag{4}$$

where

$$HK_{jk} = \int \Phi_j^*(\xi)\frac{d^2}{d\xi^2}\Phi_k(\xi)d\xi$$
$$HU_{jk} = \int \Phi_j^*(\xi)\frac{2\mu V(R)}{h\omega_e}\Phi_k(\xi)d\xi \tag{5,6}$$

Nonzero matrix elements of the HK_{jk}, are as follows:

J	k	HK_{jk}
J	j-2	$[j(j-4)/4]^{1/2}$
J	j	$(j+1/2)-(2j+1)$
J	j+2	$[(j+2)(j+1)/4]^{1/2}$

The HU_{jk} integrals were calculated numerically using the trapezoid method. The n in Eq. 3 was taken as 19 and the generated H_{ij} matrix was diagonalized for eigenvalues. Eigenfuctions were extracted from unitary transforming matrices.

The calculated relative transition moments, R_{ij}, relative transition probability, A_{ij}, relative transition intensity, I_{ij} and transition frequency, ν_{ij}, are listed in Table 4 [15]. According to Table 4, more than three transitions were expected. These may be detected with very high resolution instruments. Using a Lorenzian line shape with a 2–10 cm^{-1} full line width, three observed components in the form of IR absorption spectra were shown (Fig. 6). In Fig. 6, calculated IR intensities were utilized to construct the spectrum. The low intensity of the component at 92.9 cm^{-1} was probably the reason for its late experimental detection. Six energy levels were located in the hindered rotation area. First, three energy states were thought to be degenerate, but two stable conformations caused further splitting and, in a few, wave numbers energy levels repelled each other. However, energy levels 4–6 were opened up

Table 4 Components of the ν_2 torsional frequency (in cm^{-1})

I	j	ν_{ij}	R_{ij}	A_{ij}	I_{ij}	ν_{ij}, Experimental [17]	ν_{ij}, Experimental [18]
1	2	3.6	0.6025	0.0251	0.0251		
1	3	6.6	−0.0428	0.0002	0.0002		
1	4	100.8	−0.6602	0.8369	0.8369	104.5	102.9
1	5	127.5	0.2010	0.0981	0.0981		
1	6	133.7	0.0787	0.0158	0.0158		
1	7	203.3	0.0060	0.0001	0.0001		
2	3	3.0	4.1830	0.9940	0.9768		
2	4	97.2	−0.0986	0.0180	0.0177		
2	5	123.8	0.4354	0.4470	0.4393	124.5	125.2
2	6	130.1	−0.6163	0.9414	0.9251	124.5	125.2
2	7	199.7	0.2023	0.1557	0.1530		
3	4	94.2	−0.3035	0.1653	0.1601		92.9
3	5	120.8	0.2159	0.1073	0.1039		
3	6	127.1	0.3101	0.2330	0.2256	124.5	125.2
3	7	196.7	−0.0535	0.0107	0.0104		

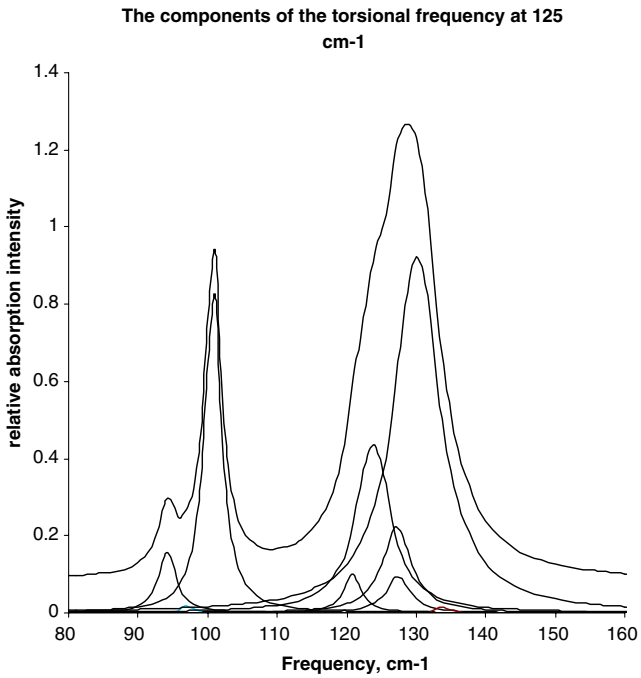

Fig. 6 The components of the torsion frequency at 125 cm^{-1}

widely and many transitions occurred among the energy levels. The seventh energy level was located above the mouth of the barrier height. This indicated that if the quantum mechanical tunneling effect happened at all, it was going to be in the 5th and 6th states (Figs. 7, 8).

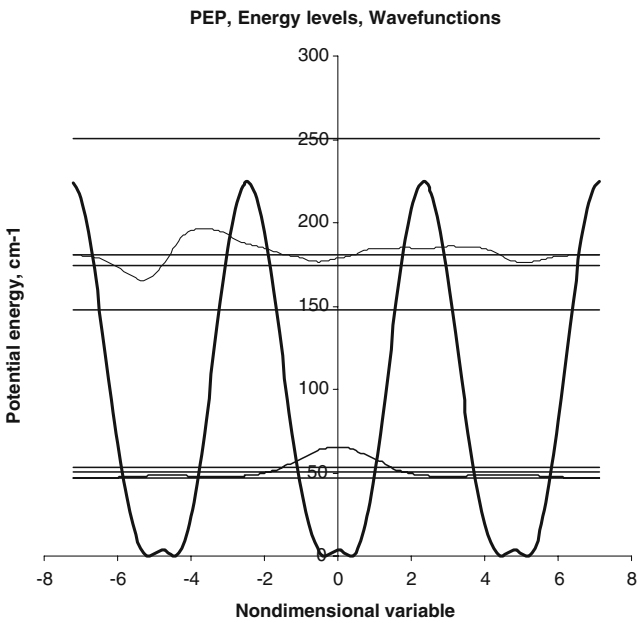

Fig. 7 PEP energy levels, first and sixth wave functions

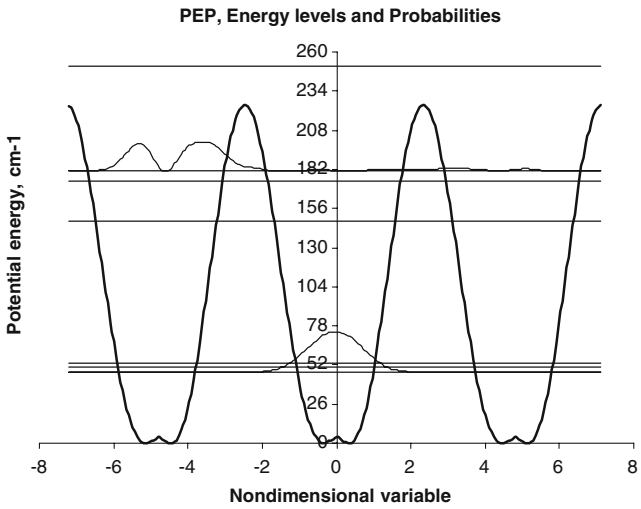

Fig. 8 PEP energy levels, first and sixth probabilities (square of the wave functions)

Conclusion

The fully relaxed model represents a more reliable physical approach to the torsion potential surface. An important outcome of this model was the significant lowering of the torsion potential barrier to 224.6 cm^{-1} from the microwave 270 cm^{-1} value. The utility of Rydberg spectroscopy in developing a torsion barrier potential model has been demonstrated. Secure ground-state ν_{12} torsion vibration frequency information allowed clear discrimination between the rigid-frame and fully relaxed models and construction of a unique ground-state empirical torsion potential.

Concerning structural properties, it was found that the length of six C–H bonds was not equal, and two methyl groups were rotated clockwise and counterclockwise about 8.5°. Potential energy and frequencies were very sensitive to the molecular geometry, hence equilibrium structures must be chosen carefully. Large and different scaling factors (often 5%–10%) were needed in harmonic oscillator consideration in different areas of the IR spectrum. In summary, we obtained the best result from an anharmonic oscillator with MP2, B3LYP with basis set 6-31G, 6-311G**.

Acetone, with its C_2v rigid frame and its C_3v methyl rotors, may be regarded as a prototype system for studying the effects of strongly coupled large amplitude motion. For this purpose, the torsion frequencies were calculated from sophisticated DFT and second order perturbation theory calculations. Correlation between the calculated and experimental spectra has allowed assignment of the major bands using the Gauss view computer program.

In this paper, the multiple structures that result from the transitions between torsion microstates have been well reproduced when compared with the available experimental data. The frequency calculated with the MP2/6-311G**

with C_1 symmetry, 139.9 cm^{-1}, was found to be slightly higher than the experimental value of 125.16 cm^{-1}. Thus, the barrier height and complex form of the PEP, which controls the torsion frequency, was calculated to be slightly higher than the value from microwave findings.

The complex form of the PEP caused the first three energy levels of the torsion to repel each other about few wave numbers, but the next three energy levels were opened up widely. The calculated transition moment provided several transitions and generated IR absorption spectra with full band width of 2–10 cm^{-1}. This showed three bands at a few cm^{-1}deviations from experimental values. The low intensity of the band at 93 cm^{-1} may be the reason for its experimentally late observation. In the future, very high resolution spectrophotometers may be able to detect other bands.

A likely explanation for the differences between the calculated and the observed frequencies could be the assumptions made in the calculations. Apart from the assumptions made in calculation, the model assumed that, while the torsion modes couple strongly with each other, they did not interact with the other modes in the molecule. The C–C–O–C molecular frame of acetone underwent skeletal vibrations. C–C–C bend at 385 cm^{-1} and C–H_2 twist at 484 cm^{-1} occurred at relatively low frequencies and could couple with the torsion modes. Interactions between either of these frame modes and the methyl tops would push and compress the torsion levels downwards and could thus account for the differences between the observed and calculated frequencies.

References

1. Smeyers YG, Senent ML, Botella V, Moule DC (1993) J Chem Phys 98:2754 doi:10.1063/1.464157
2. Ozkabak AG, Philis JG, Goodman L (1990) J Am Chem Soc 112:7854 doi:10.1021/ja00178a002
3. Jalbout AF, Basso EA, Pontes RM, Das D (2004) Theochem 167:677
4. Swalen JD, Costain CC (1959) J Chem Phys 31:1562 doi:10.1063/1.1730653
5. Peter R, Dreizler H (1965) Z Naturforsch Teil A 20:301
6. Vachhernand JM, Eijeck BP, Burie J, Demaison J (1986) J Mol Spectrosc 118:355 doi:10.1016/0022-2852(86)90175-X
7. Groner P, Gurigis GA, Durig JR (1987) J Chem Phys 86:565 doi:10.1063/1.452308
8. Gaussian 03, Revision B.01 M. J. Frisch, G. W. Trucks, H. B. Schlegel, G. E. Scuseria, M. A. Robb, J. R. heeseman, J. A. Montgomery, Jr., T. Vreven, K. N. Kudin, J. C. Burant, J. M. Millam, S. S. Iyengar, J. Tomasi, V. Barone, B. Mennucci, M. Cossi, G. Scalmani, N. Rega, G. A. Petersson, H. Nakatsuji, M. Hada, M. Ehara, K. Toyota, R. Fukuda, J. Hasegawa, M. Ishida, T. Nakajima, Y. Honda, O. Kitao, H. Nakai, M. Klene, X. Li, J. E. Knox, H. P. Hratchian, J. B. Cross, C. Adamo, J. Jaramillo, R. Gomperts, R. E. Stratmann, O. Yazyev, A. J. Austin, R. Cammi, C. Pomelli, J. W. Ochterski, P. Y. Ayala, K. Morokuma, G. A. Voth, P. Salvador, J. J. Dannenberg, V. G. Zakrzewski, S. Dapprich, A. D. Daniels, M. C. Strain, O. Farkas, D. K. Malick, A. D. Rabuck, K. Raghavachari, J. B. Foresman, J. V. Ortiz, Q. Cui, A. G. Baboul, S. Clifford, J. Cioslowski, B. B. Stefanov, G. Liu, A. Liashenko, P. Piskorz, I. Komaromi, R. L. Martin, D. J. Fox, T. Keith, M. A. Al-Laham, C. Y. Peng, A. Nanayakkara, M. Challacombe, P. M. W. Gill, B. Johnson, W. Chen, M. W. Wong, C. Gonzalez, and J. A. Pople (2003) Gaussian, Pittsburgh PA
9. Kohen W, Sham LJ (1965) Phys Rev A 140:1133 doi:10.1103/PhysRev.140.A1133
10. Vosko SH, Wilk L, Nusair M (1980) Can J Phys 58:1200
11. Becke AD (1993) J Chem Phys 98:5648 doi:10.1063/1.464913
12. Lee C, Yang W, Parr RG (1988) Phys Rev B37:785 doi:10.1103/PhysRevB.37.785
13. Moller C, Plesset MS (1934) Phys Rev 46:618 doi:10.1103/PhysRev.46.618
14. http://srdata.nist.gov/cccbdb/exp2.asp#1974sve/kov#sve/kov
15. http://srdata.nist.gov/cccbdb/exp2.asp#Shim#Shim
16. http://srdata.nist.gov/cccbdb/exp2.asp#1993Sme/Sen:2754
17. Smith DR, McKenna BK, Moller KD (1966) J Chem Phys 45:1904 doi:10.1063/1.1727869
18. Groner P, Gurirgis GA, During JR (1987) J Chem Phys 86:565 doi:10.1063/1.452308
19. Somorjai RL, Hornig DF (1962) J Chem Phys 36:1980 doi:10.1063/1.1732814